Systematic Velocity Data Reduction and its Effect on Polymer Conformation Statistics in Viscoelastic Turbulent Channel Flows

Gaurab Samanta[1], Antony N Beris[1], Robert A Handler[2] and Kostas D. Housiadas[3]

[1] *Department of Chemical Engineering, University of Delaware, Newark, DE 19716*
[2] *Naval Research Laboratory, Washington, DC 20375, USA*
[3] *Department of Mathematics, University of the Aegean, Karlovassi, Samos, Greece*

1. Introduction

Turbulent drag reduction by polymer additives is still used in energy and cost saving applications, especially in oil-pipelines. From a theoretical perspective, it is an important problem as it deals with turbulence and rheology. An in-depth understanding of this phenomenon can provide useful insights into the physics of turbulent flows. Since its discovery in 1940s, [1-3], several experimental studies, [4-7], were done to probe into the physical mechanism behind polymer-induced turbulent drag reduction. Of many theories that resulted from previous experimental investigations, viscoelastic modification of turbulence was able to explain most of the experimental observations. However, experimentally it is very difficult to explore the small scale turbulent structures. These turbulence scales are associated with higher velocity gradients which play a major role in determining the polymer conformation within the flow. With the advent of direct numerical simulation (DNS) of viscoelastic turbulent flows, it became possible to get a detailed evaluation of the structural and statistical features of the flow, [8-10].

Recent DNS work has been targeted on better understanding of the viscoelastic modification of turbulence [11-14]. Using Karhunen-Loeve (K-L) analysis of Newtonian and viscoelastic (FENE-P) channel flows at the same friction Reynolds number, Housiadas et. al. [13] showed that viscoelasticity enhances the energy stored in the larger scales of the flow. Consequently, viscoelasticity was found to suppress the smaller scales of turbulence. The enhancement of larger flow structures was also evident from flow visualizations. Handler et. al., [15] performed K-L analysis of viscoelastic turbulent channel flows DNS modeled by the Giesekus constitutive equation, and confirmed the findings of Housiadas et. al., [13]. Although, some work has been done in the field of Newtonian turbulence to study the time-dependence of large scale structures using K-L analysis [16-17], such an attempt remains elusive in viscoelastic turbulence. With this motivation and based on our previous works with K-L analysis, we undertook the study of time-dependent characteristics of the larger scales (coherent structures) in a viscoelastic turbulent channel flow using K-L analysis [18].

In short, K-L analysis provides a way to create an optimal set of orthogonal velocity eigenfunctions based on a set of independent velocity realizations [19]. The eigenfunctions are optimal in that they capture as much as possible the fluctuating kinetic energy into as few as possible eigenfunctions. Keeping this in mind, we wanted to use K-L eigenfunctions as the basis of a data reduction procedure. Hence, we embedded in our previous DNS code an extra feature to calculate projections of time-varying velocity fields generated by DNS on to a selected set of K-L velocity eigenfunctions. The selection criterion was based on how much fluctuating kinetic

energy of the flow a particular set of eigenfunctions is able to capture on an average and the cut-off was typically more than 90%. We applied this procedure in [18] to both a Newtonian and a viscoelastic case at the same friction Reynolds number and presented a comparison of the time dependent behavior of the coherent structures in these two cases. Specifically, we came up with a projection methodology and provided a preliminary analysis of the time-series of coefficients resulting from this projection. However, the impact of discarding the smaller flow scales on the turbulent statistics was not addressed in that work. In this work, we offer to address these important issues.

In particular, the polymer-chains conformation statistics is of prime importance to drag-reducing flows. Previous studies, [6-10], have shown that the deformation of polymer chains is associated with the modification of turbulence connected with drag reduction. More specifically, past investigations [8, 10, 14] led to an evaluation of statistics of the conformation (end-to-end distance of a polymer chain) tensor invariants that provided insights into the deformation behavior of polymer chains in the turbulent flow field. Hence, it is of importance to get the same statistics from the truncated (in the K-L domain) velocity information of the turbulent flow field and compare it against that calculated from the full DNS data.

2. Methods

2.1 Governing Equations and Simulation Conditions

All simulations were carried out for channel flows of a viscoelastic fluid. The viscoelastic fluid was modeled using Giesekus constitutive equation. The channel size was $L_x \times L_y \times L_z = 9 \times 2 \times 4.5$. The mesh resolution used was $N_x \times N_y \times N_z = 96 \times 96 \times 96$. A triple spectral approximation was used for every dependent variable that involved N_x Fourier modes along the streamwise periodic direction, N_z Fourier modes in the spanwise periodic direction, and $N_y + 1$ Chebyshev orthogonal polynomials along the shear direction. The drag reducing turbulent channel flow was simulated with, zero shear-rate friction Reynolds number $\mathrm{Re}_{\tau 0} = 180$, zero shear-rate friction Weissenberg number $We_{\tau 0} = 50$, and with the Giesekus model parameters, molecular extensible parameter $\alpha = 1/900$ and the ratio of the solvent viscosity to the mean total zero shear-rate viscosity at the wall $\beta_0 = 0.9$, (corresponding to the limiting Trouton ratio at infinite extensional rate of $T = 60$), with a time step of the numerical integration $\Delta t = 5 \times 10^{-4}$. These parameter values correspond to a drag reduction (DR as defined by equation 40 in [12]) of 37.4% [12].

The governing equations in dimensionless form are given as,

$$\underline{\nabla}^+ \cdot \underline{v}^+ = 0, \tag{1}$$

$$\frac{\partial \underline{v}^+}{\partial t^+} = -\underline{v}^+ \cdot \underline{\nabla}^+ \underline{v}^+ - \underline{\nabla}^+ p_p^+ + \beta_0 \underline{\nabla}^{+2} \underline{v}^+ + (1-\beta_0)\underline{\nabla}^+ \cdot \underline{\underline{\tau}}^+ + \frac{1}{Re_{\tau 0}} \underline{e}_x, \tag{2}$$

$$\frac{\partial \underline{\underline{c}}^{+}}{\partial t^{+}} + \underline{v}^{+} \cdot \underline{\nabla}^{+} \underline{\underline{c}}^{+} - \underline{\underline{c}}^{+} \cdot \underline{\nabla}^{+} \underline{v}^{+} - \left(\underline{\nabla}^{+} \underline{v}^{+} \right)^{T} \cdot \underline{\underline{c}}^{+} = -\underline{\underline{\tau}}^{+} - \alpha \underline{\underline{\tau}}^{+} \cdot \underline{\underline{\tau}}^{+} + D_0^{+} \underline{\nabla}^{+2} \underline{\underline{c}}, \tag{3}$$

$$\underline{\underline{\tau}}^{+} = \frac{\left(\underline{\underline{c}}^{+} - \underline{\underline{I}} \right)}{We_{\tau 0}}. \tag{4}$$

Here, $\underline{v}^{+}$ is the velocity vector, p_p^{+} represents the periodic component of the pressure; the non-periodic component being a linearly increasing one, driving the flow, giving rise to the separately mentioned $\left(1/Re_{\tau 0}\right)\underline{e}_x$ gradient term, with $\underline{e}_x$ representing the unit vector along the streamwise direction. $\underline{\underline{c}}^{+}$ is the conformation tensor, and D_0^{+} is the numerical diffusivity used to control the otherwise unbounded growth of the magnitudes of the resolved highest frequency modes in a hyperbolic-type conformation equation. In our DNS runs, periodicity is assumed along the average flow (streamwise) and the neutral (spanwise) directions, x, and z respectively, whereas no slip and no penetration boundary conditions are assumed for the velocity along the solid walls, perpendicular to the shearwise, y, direction.

2.2 K-L Analysis

A detailed description of the K-L decomposition method can be found in [15, 19]. Very briefly, the K-L procedure allows one to extract an optimal basis set of modes ($\underline{\psi}$) from a given database of stationary velocity realizations (here collected via DNS). The optimality is obtained by maximizing $< \left| (\underline{v}, \underline{\psi}) \right|^2 >$ (an average of the squares of the absolute value of the velocity projections) under the normalization constraint, $\left(\underline{\psi}, \underline{\psi} \right) = 1$. Here, the notation $(\cdot, \cdot)$ defines an inner-product. This results in the following eigenvalue problem,

$$\underline{\underline{L}} \cdot \underline{\psi} = \lambda \underline{\psi} \ , \tag{5}$$

where, $\underline{\underline{L}}$ is a suitable symmetric, positive definite linear operator, given in matrix form, related to the covariance matrix $\underline{\underline{R}} = \sum_{n=1}^{N} \underline{u}_{(n)} \underline{u}_{(n)}^{\dagger}$, with $\underline{u}_{(n)}, n = 1,2,..,N$ forming the database of velocity realizations on which the K-L modes are calculated. The solution to this eigenvalue problem possess a full set of orthogonal eigenfunctions (K-L eigenmodes or K-L modes) $\underline{\psi}_1, \underline{\psi}_2, ...$ corresponding to a set of positive eigenvalues, $\lambda_1, \lambda_2, ...$ that can be conveniently arranged in order of decreasing magnitude $\lambda_1 \geq \lambda_2 \geq ... \geq 0$.

Physically, the eigenvalues represent the average contribution of the corresponding K-L eigenmode to the fluctuating kinetic energy represented by the original set of velocity realizations $\underline{u}_{(n)}, n = 1,2,..,N$. This allows for a consistently better representation (uniformly convergent in the kinetic energy measure), when we project the velocities into a selected subset

of the K-L modes, $\underline{u} = \sum_{k=1}^{K} c_k \underline{\psi}_k$ as we keep increasing the number of modes involved $\underline{\psi}_k$, $k = 1,...,K, K \to \infty$ [*, *]. The K-L modes are numerically obtained in their Fourier transformed form $\underline{\hat{\psi}}_{k'}^{jl}$ with the superscripts *j*, *l* denoting the Fourier indices in the periodic *x*, *z* directions respectively and the subscript *k'* denoting the *k'th* nodal location on the *y*-axis. A selective number of the eigenmodes is then used subsequently in order to obtain a projection of the Fourier transformed velocity realizations as

$$\underline{\hat{u}}_{k'}^{jl}(t,y) = \sum_{q} a^{jlq}(t)\underline{\hat{\psi}}_{k'}^{jlq}(y) \ , \tag{6}$$

where $a^{jlq}(t)$ are the (complex in general) K-L coefficients and *q* is the quantum number index indicating the order of the eigenvalue used in the partial (for that particular Fourier mode) K-L eigenvalue analysis.

Details of the implementation of K-L viscoelastic analysis can be found in the online supplemental material provided with [15]. The K-L coefficients thus obtained and the stored selected subset of K-L eigenmodes were then used in a post-processing step as per equation (6) to reconstruct the velocity field systematically over time. These velocity realizations at different times were then subsequently used to integrate the constitutive equation in order to see if it is possible to get the conformation tensor from the K-L velocity data. The Poiseuille-type K-L mode was accounted for in the reconstruction of velocity realizations. We have varied the number of K-L coefficients (correspondingly the number of K-L modes) by setting cut-offs on the minimum eigenvalue of any K-L mode to be selected to reconstruct back the velocity fields so that the effect of this variation can be studied. Statistically independent realizations of the reconstructed velocity and conformation fields were stored for the subsequent calculation of statistics.

3. Results and Discussion

3.1. Influence of K-L data reduction on velocity statistics

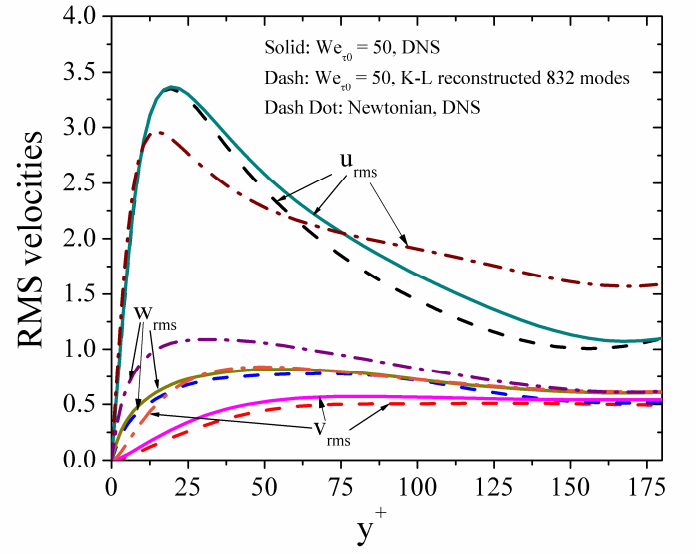

(a)

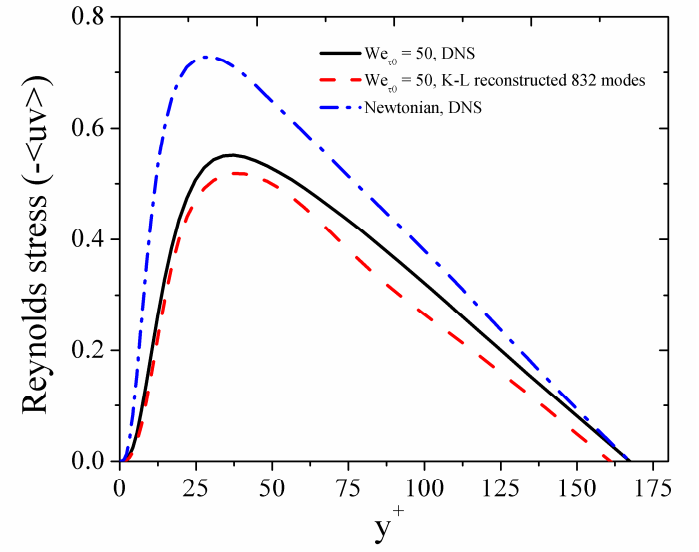

(b)

Fig. 1: (a) Root mean square velocity component fluctuations as a function of y^+. (b) Reynolds shear stress (xy-component) as a function of y^+. Solid lines represent results from viscoelastic ($We_{\tau 0} = 50$) DNS, dashed lines represent corresponding results from K-L reconstruction using 832 modes, and dash-dotted lines represent results from Newtonian DNS.

Figure 1 shows comparisons between the velocity statistics obtained from a full DNS and a K-L reconstructed case. From figure 1(a), we can see that the r.m.s. values of the velocity fluctuations corresponding to the viscoelastic K-L reconstructed case with 832 K-L modes (subject to the selection criterion $\lambda > 10^{-3}$) are in good agreement with the corresponding DNS r.m.s. values for all the components. In particular, there is no difference in the r.m.s. values of streamwise velocity fluctuations between these two cases until the peak value is attained, after

which the r.m.s. values for the K-L reconstructed case fall slightly (with a maximum fall of around 15%) before again meeting the DNS values near the channel center. As shown in figure 1(b), the Reynolds stress values corresponding to the K-L reconstructed data are close to their corresponding DNS values near the wall, with differences occurring from the peak onwards towards the channel center (with a maximum reduction of about 15%). Therefore, quite clearly the K-L reconstruction using just 832 high energy K-L modes gives a good representation of the velocity statistics especially close to the wall.

3.2. Influence of K-L data reduction on conformation statistics

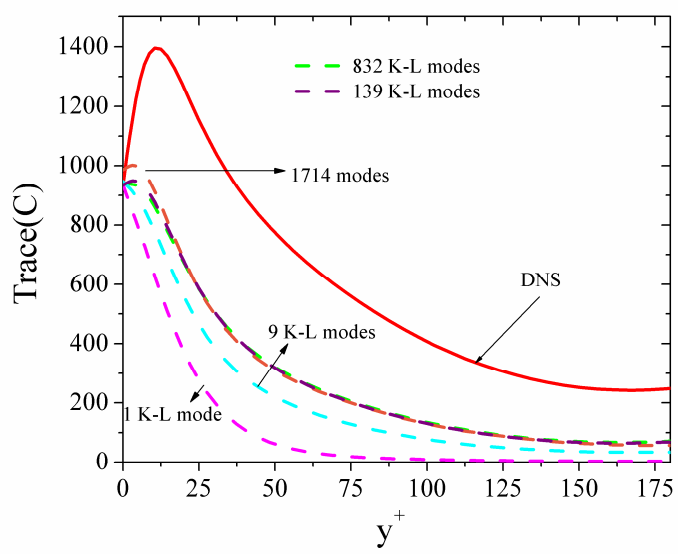

Fig. 2: Time-averaged trace of conformation tensor as a function of y^+ for viscoelastic turbulent channel flow with $We_{\tau 0} = 50$. Solid line represents DNS results while dashed lines represent results from various K-L reconstructions.

In figure 2, we compare conformation trace statistics from a number of K-L reconstruction cases with varying number of K-L modes against those obtained from a full DNS. Failure to match the DNS results is obvious. Even with the K-L coefficients retrieved from projections onto 1714 K-L modes (which is the maximum that we had at hand), we were able to reproduce only about 50% of the trace corresponding to the maximum molecular extension observed near the buffer layer. Most importantly, the physically relevant peak at the buffer region is lost in all but the larger K-L reconstructed cases and even there it is barely discernible. This peak however in the conformation trace offers considerable evidence on the role of the extensional deformation in stretching the polymer chains that is believed to be intimately linked to drag reduction [8, 10]. This is related to the increased extensional viscosity of the polymers which many previous studies have considered to be the prime reason behind drag reduction [8, 10, 12, 13, and 20].An interesting observation from the plot in figure 2 is that there is a seemingly saturation effect of the number of K-L modes on the trace statistics in the reconstruction cases. Increasing the number of K-L modes beyond 139 shows very little improvement in the trace statistics. The discrepancies observed in trace plot can be linked to the severe truncation applied on the number of K-L modes, keeping only high energy, large-scale structures for reconstruction. This also supports the saturation effect observation where it is

possible that if we use a sufficiently large number of K-L modes, we will keep progressing towards the DNS results. However, that will be at the cost of using a very large number of K-L modes which will defeat the purpose of developing a data-reduction model. That is to say, to properly approach a data-reduction model of a turbulent drag-reducing viscoelastic flow, one needs to account for the small-scale turbulence that is closely linked to polymer conformation in the flow field. To accomplish this, we came up with a modification to the K-L procedure.

In the new method, instead of maximizing $<\left|(\underline{v},\underline{\psi})\right|^2>$ under the normalization constraint $\left(\underline{\psi},\underline{\psi}\right)=1$, we maximize $\frac{1}{N}\sum_{n=1}^{N}\left(\sum_{m=1}^{3}\left\langle\nabla_m \underline{v},\nabla_m \underline{\psi}\right\rangle\right)^2$ under the constraint of normalization given by $\left|\sum_{m=1}^{3}\left\langle\nabla_m \underline{\psi},\nabla_m \underline{\psi}\right\rangle\right|=1$. Essentially, in the new procedure, we are maximizing the average of the squares of the projections of velocity gradients onto gradients of the eigenfunctions. This way, we are able to preserve the linear characteristics of the eigenvalue problem. The solution to this eigenvalue problem results in Laplacian (∇^2) of the eigenfunctions optimally capturing the fluctuating dissipation in a linear sense. Therefore, we called it the "Dissipative-KL" analysis.

In a preliminary attempt, we implemented the Dissipative-KL analysis to create a selected set of top dissipative modes. This selection was based on the eigenvalues of those modes. Then as previously, we used this selected set of modes to obtain projection coefficients by projecting velocities from a DNS onto them. The selected set of dissipative modes and the projection coefficients were then used, as earlier, to reconstruct velocity fields over time. The conformation trace statistics obtained from the independent conformation realizations, gathered after utilizing the reconstructed velocity fields to integrate the constitutive equation, is shown in figure 3. The physically relevant peak in the buffer region is much more pronounced now and overall the results are closer to the DNS. Hence, the dissipative-KL analysis holds promise for properly accounting for the smaller (dissipative) scales of turbulence in order to preserve the right conformation statistics, as obtained from a DNS.

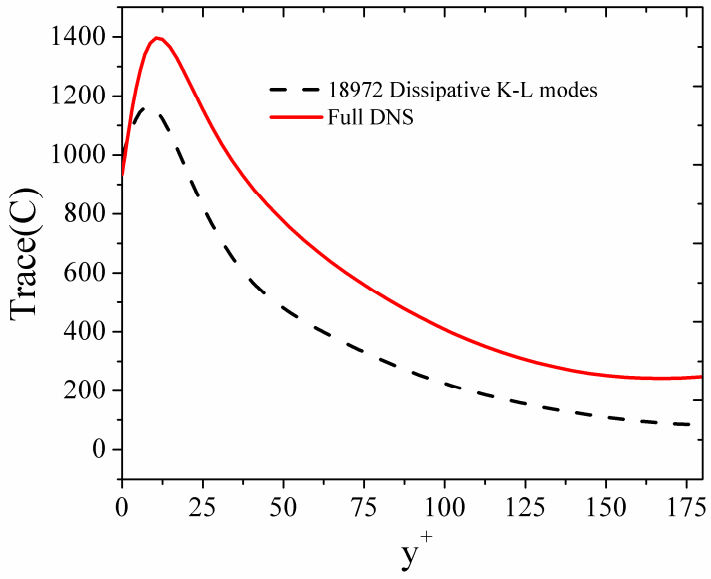

Fig. 3: Time-averaged trace of conformation tensor as a function of y^+ for viscoelastic turbulent channel flow with $We_{\tau 0} = 50$. Solid line represents DNS results while the dashed line represents result from the Dissipative-KL reconstruction.

4. Conclusions

The K-L analysis serves as a useful tool to approximate velocity statistics of a viscoelastic turbulent channel flow. However, it fails to deliver good physically meaningful results so far as conformation trace statistics are concerned. As the conformation trace is closely linked to the drag reduction mechanism in such flows, proper accountability of it is required for developing a data-reduction model of these flows. A new method called "Dissipative-KL analysis" was devised to properly account for the conformation trace statistics. Preliminary results for this method show substantial improvement in the conformation trace statistics. An investigation is still underway to test the performance of this new method, either separately or in conjunction with K-L analysis, in order to develop a data-reduction model for viscoelastic turbulent channel flows.

Acknowledgments

One of the authors (GS) would like to acknowledge the financial support provided by the Department of Chemical Engineering, University of Delaware. We are also grateful to the National Center for Supercomputing Applications (NCSA) for providing the computational resources needed for this work through an Alliance proposal grant MCA96N005P

References

[1] B. A. Toms, Observations on the flow of linear polymer solutions through straight tubes at large Reynolds numbers, *Proc. 1st Intern. Congr. Rheol*., **2** (1948), 135-141.

[2] K.J. Mysels, Flow of thickened fluids, *U.S. Pattent* **2,492,173**, (1949).

[3] J. G. Oldroyd, A suggested method of detecting wall effects in turbulent flow through pipes, *Proc. 1st Intern. Congr. Rheol*., **2** (1948), 130-134.

[4] A. B. Metzner, and M. G. Park, Turbulent flow characteristics of viscoelastic fluids, *J. Fluid Mech*., **20** (1964), 291-303.

[5] P. S. Virk, E. W. Merrill, H. S. Mickley, K. A. Smith, and E. L. Mollo-Christensen, The Toms phenomenon: turbulent pipe flow of dilute polymer solutions, *J. Fluid Mech*., **30** (1967), 305-328.

[6] T. S. Luchik, and W. G. Tiederman, Turbulent structure in low-concentration drag-reducing channel flows, *J. Fluid Mech*., **190** (1988), 241-263.

[7] J. L. Lumley, Drag reduction by additives, *Ann. Rev. Fluid Mech*., **1** (1969), 367-384.

[8] R. Sureshkumar, A. N. Beris, and R. A. Handler, Direct numerical simulation of the turbulent channel flow of a polymer solution, *Phys. Fluids*, **9** (1997), 743-754.

[9] T. Min, J. Y. Yoo, H. Choi, and D.D. Joseph, Drag reduction by polymer additives in a turbulent channel flow, *J. Fluid Mech*., **486** (2003), 213-238.

[10] C. D. Dimitropoulos, R. Sureshkumar, and A. N. Beris, Direct numerical simulation of viscoelastic turbulent channel flow exhibiting drag reduction: effect of the variation of rheological parameters, *J. Non-Newtonian Fluid Mech.*, **79** (1998), 433-468.

[11] K. D. Housiadas, and A. N. Beris, Polymer-induced drag reduction: Effects of the variations in elasticity and inertia in turbulent viscoelastic channel flow, *Phys. Fluids*, **15** (2003), 2369-2384.

[12] K. D. Housiadas, and A. N. Beris, An efficient fully implicit spectral scheme for DNS of turbulent viscoelastic channel flow, *J. Non-Newtonian Fluid Mech*., **122** (2004), 243-262.

[13] K. D. Housiadas, and A. N. Beris, and R. A. Handler, Viscoelastic effects on higher order statistics and on coherent structures in turbulent channel flow, *Phys. Fluids*, **17** (2005), 035106 (20 pages).

[14]T. Vaithianathan, A. Robert, J.G. Brasseur ,and L.R. Collins, An improved algorithm for simulating three-dimensional, viscoelastic turbulence, *J. Non-Newtonian Fluid Mech*., **140** (2006), 3-22.

[15] R. A. Handler, K. D. Housiadas, and A. N. Beris, Karhunen-Loeve representations of drag reduced turbulent channel flows using the method of snapshots, *Int. J. Numer. Meth. Fluids*, **52** (2006), 1339-1360.

[16] S. Sanghi, and N. Aubry, Mode interaction models for near wall turbulence, *J. Fluid Mech.*, **247** (1993), 455-488.

[17] G. A. Webber, R. A. Handler, and L. Sirovich, Energy dynamics in a turbulent channel flow using the Karhunen-Loeve approach, *Int. J. Num. Meth. Fluids*, **40 (**2002), 1381-1400.

[18] G. Samanta, G.M. Oxberry, A. N. Beris, R. A. Handler, and K. D. Housiadas, Time-evolution K-L analysis of coherent structures based on DNS of turbulent Newtonian and viscoelastic flows, *J. Turbulence (accepted)*, 2008.

[19] P. Holmes, J. L. Lumley, and G. Berkooz, Turbulence, coherent structures, dynamical systems and symmetry, *Cambridge Univ. Press*, Cambridge (1996).

[20] B. Yu, and Y. Kawaguchi, Effect of Weissenberg number on the flow structure: DNS study of drag reducing flow with surfactant additives, *Int. J. Heat Fluid. Trans*., **24 (**2003), 491-499.